

Electron—noble-gas spin-flip scattering at low energy

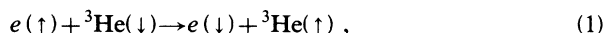
T. G. Walker, K. Bonin, and W. Happer

Department of Physics, Princeton University, Princeton, New Jersey 08544

(Received 1 December 1986)

The spin-exchange rates and spin-relaxation rates for thermal electrons colliding with noble-gas atoms are calculated using the orthogonalized-plane-wave approximation and via partial-wave analysis. The two techniques give similar results and are in order-of-magnitude agreement with the experimental rate in Ar.

The spin-exchange and relaxation properties of free electrons are of interest in situations where spin-polarized species (e.g., Rb, Ba⁺, ³He) are studied in the presence of electrons; examples include optically pumped Ba⁺e⁻ plasmas and ionization in spin-polarized gaseous targets. There is considerable interest in nuclear¹ and medium-energy physics in producing polarized ³He and one of several possible processes for doing this is spin exchange with a reservoir of polarized electrons. In this paper we calculate the electron-nuclear spin-exchange rates for electrons colliding with neutral noble-gas atoms, e.g., a process such as



where the arrows denote the directions of the electron and nuclear spins. We also calculate the spin-orbit relaxation rates for the process



for all the noble gases He, Ne, Ar, Kr, Xe, and Rn. We assume that the electron temperature is sufficiently low that only *s*- and *p*-wave scattering need be considered.

The process given by (1) proceeds via the Fermi contact interaction

$$V_{\text{FC}} = \frac{16\pi}{3} \frac{\mu_B \mu_K}{K} \delta(\mathbf{r}) \mathbf{S} \cdot \mathbf{K} \quad (3)$$

between the density of electronic spin **S** at the site **r**=0 of the noble-gas nuclear spin **K**. The Bohr magneton and the nuclear moment are denoted by μ_B and μ_K , respectively. Process (2) is due to the spin-orbit interaction

$$V_{\text{SO}} = \frac{\hbar^2}{2mc^2} \frac{1}{r} \frac{dV}{dr} \mathbf{S} \cdot \mathbf{L} \quad (4)$$

where **L** is the orbital angular momentum of the free electron, *m* is the electron mass, and *V* is the shielded Coulomb potential of the noble gas core. Using the distorted-wave Born approximation (DWBA), we show that the rates per noble-gas atom for processes (1) and (2) are

$$\frac{1}{\tau_{\text{FC}}} = \frac{256}{27\hbar^4} (2\pi m^3 kT)^{1/2} \left[\frac{\mu_B \mu_K}{K} \right]^2 \eta_0^4 K(K+1) \quad (5)$$

and

$$\frac{1}{\tau_{\text{SO}}} = \frac{64(2\pi)^{1/2}}{3} \frac{m^{7/2}}{\hbar^6} (kT)^{5/2} (G/h)^2 \quad (6)$$

for an electron gas of temperature *T*. The factors η_0 and *G* in (5) and (6) are constants characteristic of the noble gas; we show that in the orthogonalized-plane-wave (OPW) approximation² η_0 and *G* are the same constants used to calculate the electron-nuclear spin-exchange interaction and spin-rotation interaction of alkali-metal—noble-gas atomic pairs.³

To obtain (5) and (6) we assume the problem of spin-independent scattering of the electron in the potential of the atom has been solved and the electron wave function is

$$\psi_{\mathbf{k}}(\mathbf{r}) = 4\pi \sum_{l=0,1} i^l k^l \eta_l \frac{P_l(r)}{r} \mathbf{Y}_l(\hat{\mathbf{k}}) \cdot \mathbf{Y}_l(\hat{\mathbf{r}}). \quad (7)$$

Here the functions $P_l(r)$ are solutions of the radial Schrödinger equation in the scattering potential *V*. The behavior of $P_l(r)$ at small *r* is chosen such that $\eta_l = 1$ for *V*=0:

$$P_l(r) \xrightarrow{r \rightarrow 0} \frac{r^{l+1}}{(2l+1)!!}.$$

Then η_0 and η_1 represent the enhancement, due to the noble-gas potential, of $\psi(0)$ and $\psi'(0)$ with respect to the free-electron case. We consider only *l*=0,1 and so low energies are assumed. The matrix element of (3) in the DWBA for a transition between an initial state of electron momentum $\hbar\mathbf{k}_i$, electron-spin quantum number $m_s = \frac{1}{2}$, and nuclear-spin quantum number m_K to a final state of electron momentum $\hbar\mathbf{k}_f$, electron spin quantum number $m_s = -\frac{1}{2}$ and nuclear spin quantum number $m_K + 1$ is

$$\begin{aligned} \langle f | V_{\text{FC}} | i \rangle &= \psi_{\mathbf{k}_f}^*(0) \psi_{\mathbf{k}_i}(0) \frac{8\pi}{3} \frac{\mu_B \mu_K}{K} \\ &\times [K(K+1) - m_K(m_K+1)]^{1/2} \delta_{\mathbf{k}_f, \mathbf{k}_i} \\ &= |\eta_0|^2 \frac{8\pi}{3} \frac{\mu_B \mu_K}{K} [K(K+1) \\ &\quad - m_K(m_K+1)]^{1/2}, \quad (8) \end{aligned}$$

where $\eta_0 = \psi_{k_i}(0) = \psi_{k_f}(0)$ and the corresponding matrix element of (4) is

$$\langle f | V_{SO} | i \rangle = i \frac{G}{2} (\mathbf{k}_i \times \mathbf{k}_f) \cdot (\hat{\mathbf{x}} + i\hat{\mathbf{y}}), \quad (9)$$

where

$$G = 6\pi\eta_1^2 \frac{\hbar^2}{m^2c^2} \int P_1^2 \frac{1}{r} \frac{dV}{dr} dr \quad (10)$$

and $\hat{\mathbf{x}}$ and $\hat{\mathbf{y}}$ are unit vectors along the x and y axes.

Averaging over an initially unpolarized gas of nuclei and a Boltzmann distribution of electron energies, (8) and (9) give (5) and (6). The calculation of the factors G and η_0 requires a knowledge of $\psi_{\mathbf{k}}$. We will calculate $\psi_{\mathbf{k}}$ using both the OPW and partial-wave (PW) techniques and compare the results.

In the OPW approximation, we orthogonalize the free-electron wave function

$$e^{i\mathbf{k}\cdot\mathbf{r}} \simeq 1 + i\mathbf{k}\cdot\mathbf{r}$$

to the occupied core orbitals of the noble gas:

$$\psi_{\mathbf{k}} \simeq 1 + i\mathbf{k}\cdot\mathbf{r} - \sum_n C_{ns} \phi_{ns}(\mathbf{r}) - \sum_n C_{np} \mathbf{k}\cdot\phi_{np}(\mathbf{r}), \quad (11)$$

where

$$\phi_{np} = \phi_{np_x} \hat{\mathbf{x}} + \phi_{np_y} \hat{\mathbf{y}} + \phi_{np_z} \hat{\mathbf{z}} \quad (12)$$

is a Cartesian vector formed from the p orbitals, and

$$C_{ns} = \int_0^\infty \phi_{ns}(\mathbf{r}) d^3\mathbf{r} \quad (13)$$

and

$$C_{np} = \int_0^\infty z \phi_{np}(\mathbf{r}) d^3\mathbf{r}. \quad (14)$$

Many convenient core orbitals ϕ_{ns} and ϕ_{np_z} can be found in the literature and we have used the values published by Herman and Skillman.⁴ Thus

$$\psi_{\mathbf{k}}(0) = 1 - \sum_n C_{ns} \phi_{ns}(0) = \eta_0 = \eta \quad (15)$$

which is R. Herman's equation⁵ for the spin enhancement factor η . Likewise, equating the p -wave parts of (11) and (7),

$$\eta_1 \frac{P_1}{r} = \frac{r}{3} - \sum_n \frac{C_{np}}{(12\pi)^{1/2}} \frac{R_{np}}{r} \simeq - \sum_n \frac{C_{np}}{(12\pi)^{1/2}} \frac{R_{np}}{r} \quad (16)$$

gives

$$G = 1/2 (\hbar/mc)^2 \int_0^\infty \left(\sum_n C_{np} R_{np} \right)^2 \frac{1}{r} \frac{dV}{dr} dr, \quad (17)$$

where

$$\phi_{np_z} = \left(\frac{3}{4\pi} \right)^{1/2} \frac{R_{np}}{r^2} Z,$$

identical to the relation in Ref. 3. Values of G/h and η are listed in Table I. The OPW method gives a simple result which is easily calculable from the published tables of

TABLE I. Comparison of η and G calculated via the OPW method and the PW method. The Rn results assume an s -wave scattering length of -5.1 \AA .

Atom	η		G/h ($10^{-31} \text{ MHz cm}^5$)	
	OPW	PW	OPW	PW
He	-9.5	-5.3		2.4×10^{-4}
Ne	15	9.4	0.062	0.028
Ar	-21	-22	0.49	0.25
Kr	35	44	3.0	1.5
Xe	-50	-73	9.8	6.0
Rn	63	114	31	30

atomic wave functions.

The OPW method cannot be used to calculate G for He due to the lack of occupied p orbitals in the ground state of the atom, so we have used a PW analysis to calculate G for He. For other noble gases the PW analysis serves to give an indication of the reliability of the results (10) and (11). PW analysis requires a knowledge of the potential V seen by an external electron scattering off the atom. The tabulated Herman-Skillman potential V_0 is the potential seen by an electron internal to the neutral atom, and therefore behaves as $1/r$ for larger r . The true behavior of V for large r should be $-ae^2/2r^4$, where α is the atomic polarizability and e the electron charge. To obtain a physically reasonable potential V we added two terms to V_0 :

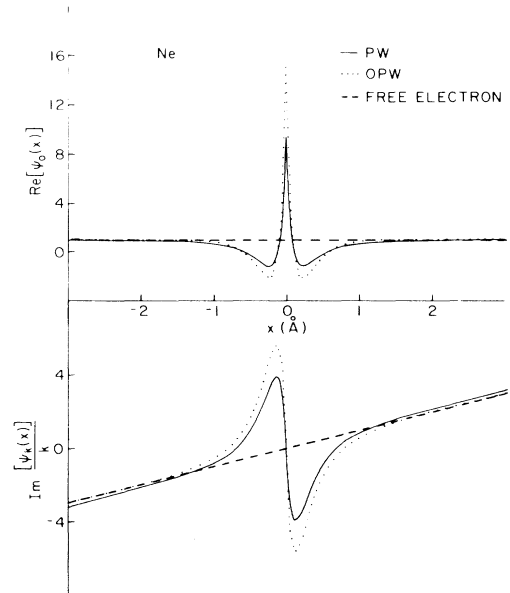


FIG. 1. Cross-sectional plots of $\text{Re}(\psi)$ (s -wave) and $\text{Im}(\psi/k)$ (p -wave) for Ne at zero energy, for the partial-wave (PW) and orthogonalized-plane-wave (OPW) approximations. Also shown, for comparison, are the corresponding free-electron wave functions.

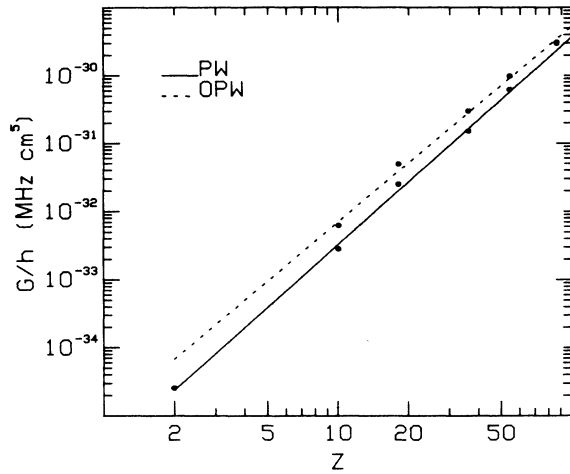


FIG. 2. The characteristic constant G/h as a function of atomic number Z as calculated by the orthogonalized-plane-wave (OPW) and partial-wave (PW) approximations. The fits are $G = 9.34 \times 10^{-36} Z^{2.88}$ for the OPW results and $G = 2.89 \times 10^{-36} Z^{3.06}$ for the PW calculations.

$$V_1 = \frac{\alpha e^2}{2r^4} (1 - e^{-r/r_0})^5 \quad (18)$$

and

$$V_2 = \frac{e^2}{r} \sum_{n,l} \frac{2(2l+1) \int_0^r R_{nl}^2(r') dr'}{Z}$$

V_1 is the usual polarizability potential multiplied by a function which goes to zero inside the atom, and V_2 shields the $1/r$ behavior of V_0 for large r . The parameter r_0 in (18) was adjusted to reproduce the s -wave scattering lengths deduced from experiment by O'Malley,⁶ so although there is a certain arbitrariness in the functional form of V_1 and V_2 , the total potential V gives the correct scattering cross sections for slow electrons.

The radial Schrödinger equation

$$\frac{-\hbar^2}{2m} \frac{d^2 P_l}{dr^2} + \left[V + \frac{\hbar^2 l(l+1)}{2mr^2} \right] P_l = 0$$

was integrated out from $r=0$ and matched to the ap-

TABLE II. Comparison of experimental spin-relaxation times and cross sections with the orthogonalized plane-wave approximation and partial-wave analysis.

Atom	Experiment	Theory	
	σ_{SO}^a or τ_{SO}^b	OPW	PW
He	$< 1.5 \times 10^{-22}$ cm ²		3.5×10^{-29} cm ²
Ne	$< 1.6 \times 10^{-22}$ cm ²	4.9×10^{-24} cm ²	1.0×10^{-24} cm ²
Ar	$< 5.3 \times 10^{-21}$ cm	1.5×10^{-24} cm ²	3.8×10^{-23} cm ²
	6×10^{-5} sec	2×10^{-4} sec	8×10^{-4} sec
Kr	$< 1.6 \times 10^{-20}$ cm ²	5.4×10^{-21} cm ²	1.4×10^{-21} cm ²
Xe	$< 2.6 \times 10^{-20}$ cm ²	5.5×10^{-20} cm ²	2.2×10^{-20} cm ²

^aReference 9.

^bReference 8.

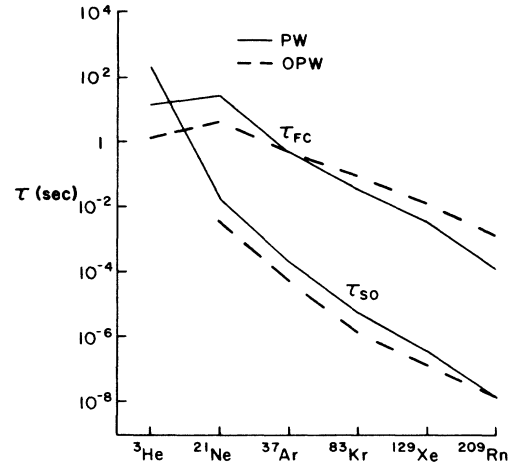


FIG. 3. Expected spin-relaxation times due to the Fermi contact (FC) interaction and the spin-orbit (SO) interaction.

propriate asymptotic forms of the wave function.⁶ The matching conditions give η_0 and η_1 . We have graphed $\text{Re}(\psi_0)$ and $\text{Im}(\psi_k/k)$ for Ne obtained in this way in Fig. 1, along with analogous results for the OPW. It is seen that the OPW does well inside the core of the noble gas, but does not account at all for the scattered wave. The results for η_0 and G are given in Table I. Figure 2 shows the results for G as a function of Z . Note that G is closely approximated by $G = AZ^n$, where $n = 2.88$ for the OPW case and $n = 3.06$ for the partial-wave case. All results agree within a factor of 2.5 for the two methods. The partial-wave results could be made more accurate by using a more realistic potential—the Herman-Skillman potential is known to give poor results for phase shifts.⁷ The OPW technique could be improved by adding in the wave-function perturbations due to the pseudopotential, but the zeroth-order results (15) and (17) are adequate for these order-of-magnitude estimates.

The OPW method works well for the present calculations because the interactions (3) and (4) are localized inside the core of the noble gas, where the OPW best approximates the true wave function. The OPW method

TABLE III. Predicted electron spin-relaxation times τ_{FC} and τ_{SO} using OPW and PW results for G and η , at noble-gas temperature $T_0 = 300$ K and pressure $p_0 = 1$ atm. τ_{FC} scales as $(p_0/p)(T/T_0)^{1/2}$ and τ_{SO} scales as $(p_0/p)(T_0/T)^{3/2}$.

Atom	τ_{FC} (sec)		τ_{SO} (sec)	
	OPW	PW	OPW	PW
³ He	1.5	15		2×10^2
²¹ Ne	4.3	28	3.4×10^{-3}	1.6×10^{-2}
³⁷ Ar	0.50	0.50	5.4×10^{-5}	2.1×10^{-4}
⁸³ Kr	9.3×10^{-2}	3.7×10^{-2}	1.4×10^{-6}	5.6×10^{-6}
¹²⁹ Xe	1.4×10^{-2}	3.2×10^{-3}	1.4×10^{-7}	3.4×10^{-7}
²⁰⁹ Rn	1.4×10^{-3}	1.3×10^{-4}	1.4×10^{-8}	1.4×10^{-8}

completely fails to account for scattering unless further perturbations due to the pseudopotential are added in.

The rate for the process (2) was measured by Dehmelt⁸ for electrons in Ar gas. He obtained $\tau_{SO} = 6 \times 10^{-5}$ sec for an Ar number density of $2.5 \times 10^{18} \text{ cm}^{-3}$ and the electron temperature $> 140^\circ\text{C}$. Equation (6) gives 2×10^{-4} sec for the OPW approximation and 8×10^{-4} sec for the partial wave analysis at 140°C . The presence of an rf field in Dehmelt's experiment heated the electrons to a temperature greater than the 140°C ambient temperature, and the $T^{5/2}$ dependence in (6) means that a 90°C increase in the electron temperature brings down the OPW theoretical prediction of τ_{SO} to 1.2×10^{-4} sec, a factor of 2 larger than experiment. Experimental upper limits on $\sigma_{SO} = 1/\tau_{SO}v$ have been estimated by Weber *et al.*⁹ Table II shows these limits, along with values calculated from (6) and (17). The calculations are consistent with the experimental limits. In Fig. 3 we graph τ_{SO} and τ_{FC} versus noble gas. Note that for ^3He , the Fermi contact interaction (1) dominates while the spin-orbit interaction of (2) dominates for the other noble gases.

The agreement between calculations based on orthogonalized orbitals and measured values of the electron-nuclear spin-exchange coupling constant (proportional to η_0^2) and the spin-rotation coupling constant (proportional to G) in alkali-metal-noble-gas van der Waals molecules³ supports the assumption that the orthogonalization pro-

cedures give a good approximation to the electron wave function in the core of the noble gas. Also note the extremely small spin-orbit cross sections for He and Ne. These imply electron spin relaxation times at room temperature in one atmosphere of He and Ne gas of 200 and 0.017 sec, respectively. Predicted electron spin-relaxation times for all the noble gases are given in Table III.

The temperature dependence of (6) is a striking signature of the process (2). One could envision heating a plasma of e^- and Ba^+ in He via microwaves⁹ and hence making (2) much larger than in the relatively cool discharges of Ref. 7, thus making (6) more easily observable.

In conclusion, we have shown that the spin-flip scattering of electrons off noble gases can be simply estimated using the OPW technique or by partial waves and the estimates are consistent with each other. The interactions are so small for thermal electrons in ^3He or ^4He that in practice the spin relaxation of thermal electrons in He must be dominated by other mechanisms, for example, diffusion to the walls, spin exchange with positive ions, or recombination.

ACKNOWLEDGMENT

This work was supported under Grant No. DAAG-29-83-K-0072 from the U.S. Army Research Office.

¹Workshop on Polarized ^3He Beams and Targets, edited by R. W. Dunford and F. P. Calaprice (AIP, New York, 1985).

²M. H. Cohen and V. Heine, *Phys. Rev.* **122**, 1821 (1961).

³Z. Wu, T. G. Walker, and W. Happer, *Phys. Rev. Lett.* **54**, 1921 (1985).

⁴F. Herman and S. Skillman, *Atomic Structure Calculations* (Prentice Hall, Englewood Cliffs, N.J., 1961).

⁵R. M. Herman, *Phys. Rev.* **137**, A1062 (1965).

⁶T. F. O'Malley, *Phys. Rev.* **130**, 1020 (1963).

⁷K. C. Pandey, Sudhanshu S. Jha, and J. A. Armstrong, *Phys. Rev. Lett.* **44**, 1583 (1980).

⁸H. G. Dehmelt, *Phys. Rev.* **109**, 381 (1958).

⁹E. W. Weber, *Phys. Rep.* **32**, 123 (1977).